Electronic Supplementary Material (ESI) for Journal of Materials Chemistry B.
This journal is © The Royal Society of Chemistry 2022

Supporting Information

Enhanced Photothermal Heating and Combination Therapy of NIR Dye via Conversion to Self-Assembled Ionic Nanomaterials

Samantha Macchi[a], Amanda Jalihal[a], Nasrin Hooshmand[b], Mohd Zubair[c], Nabeel Alwan[1], Mostafa El Sayed[b], Nawab Ali[c], Robert J. Griffin,[d] and Noureen Siraj[a]*

[a] *Department of Chemistry, University of Arkansas at Little Rock, Little Rock, AR 72022, USA*

[b] *Laser Dynamics Laboratory, School of Chemistry and Biochemistry, Georgia Institute of Technology, Atlanta, Georgia 30332-0400, United States of America*

[c] *Department of Biology, University of Arkansas at Little Rock, Little Rock, AR 72022, USA*

[d] *University of Arkansas for Medical Sciences, Winthrop P. Rockefeller Cancer Institute, Arkansas Nanomedicine Center, Department of Radiation Oncology, 4301 W Markham St, Little Rock, AR 72205, USA*

*Corresponding author: (E) nxsiraj@ualr.edu (O) 501-569-8829

Synthetic procedure for IR783-based IM

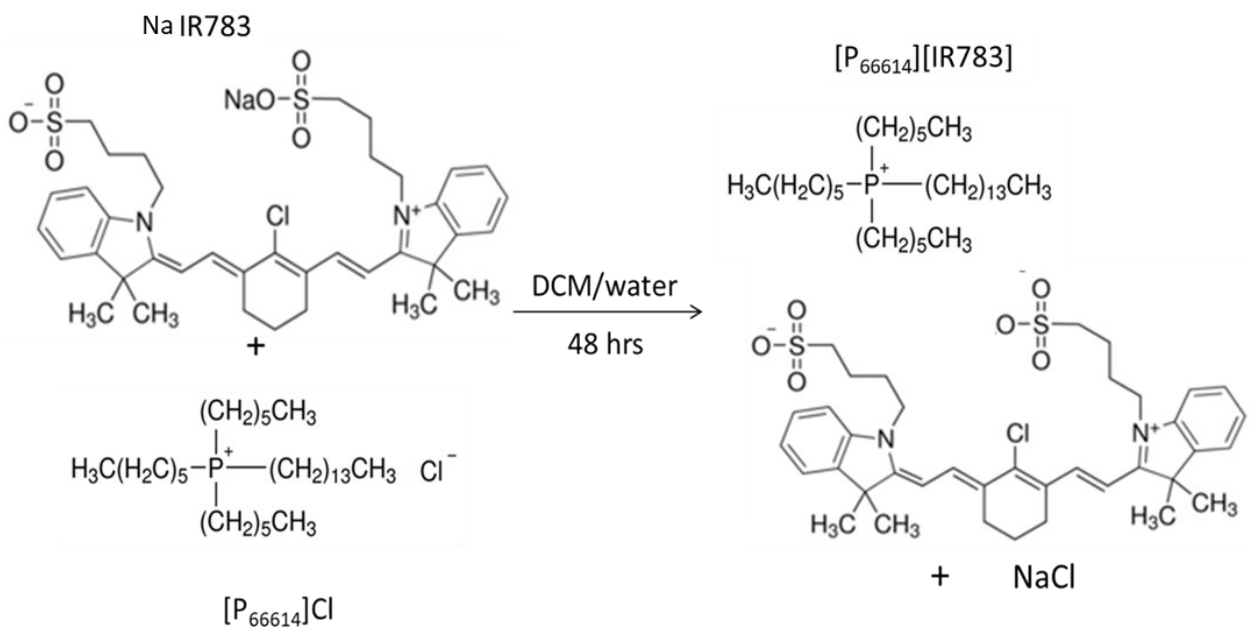

Scheme S1. Synthetic procedure for $[P_{66614}][IR783]$ ionic material

Characterization of IMs

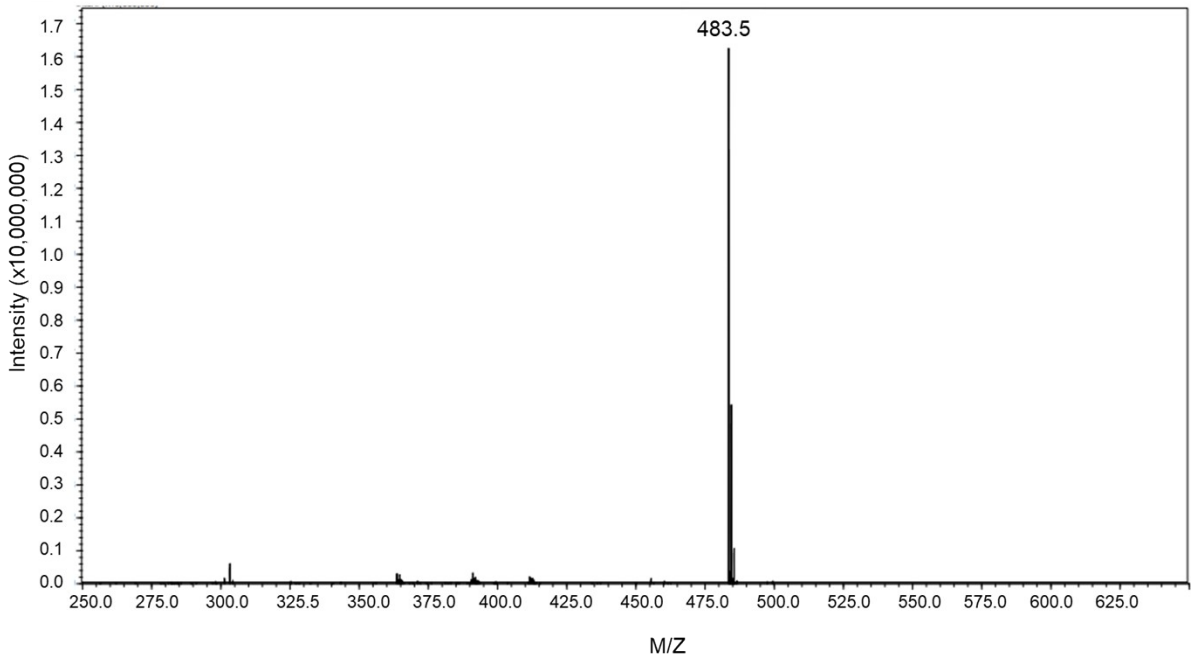

Figure S1. Mass spectrum in positive ion mode for $[P_{66614}][IR783]$

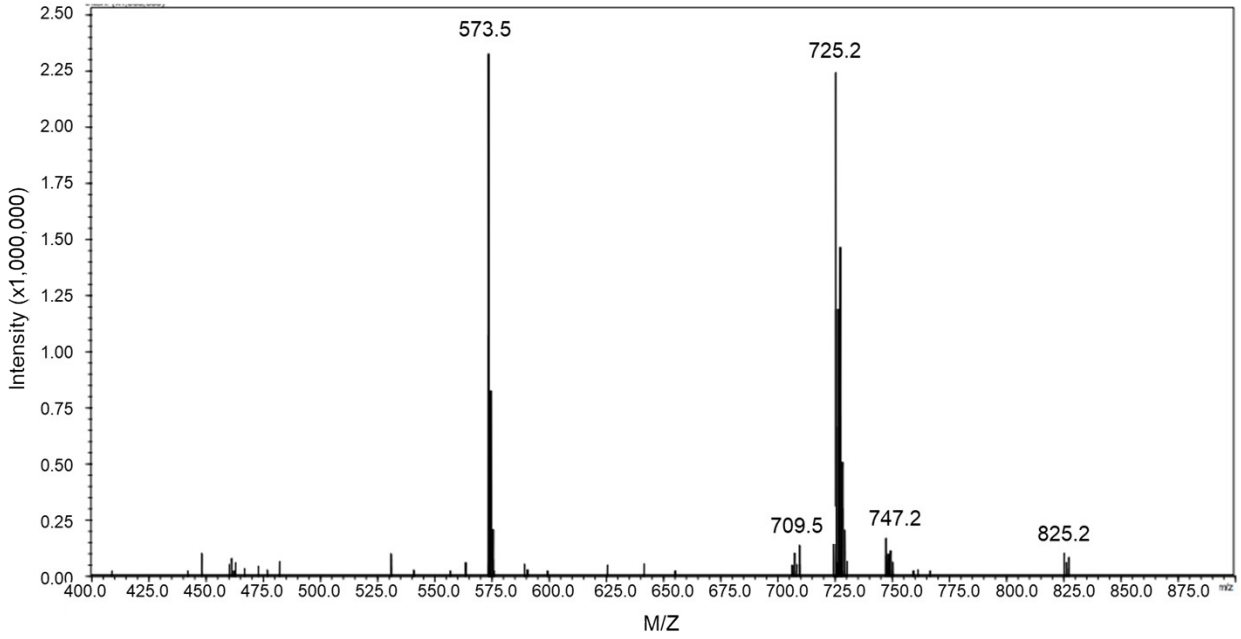

Figure S2. Mass spectrum in negative ion mode for $[P_{66614}][IR783]$

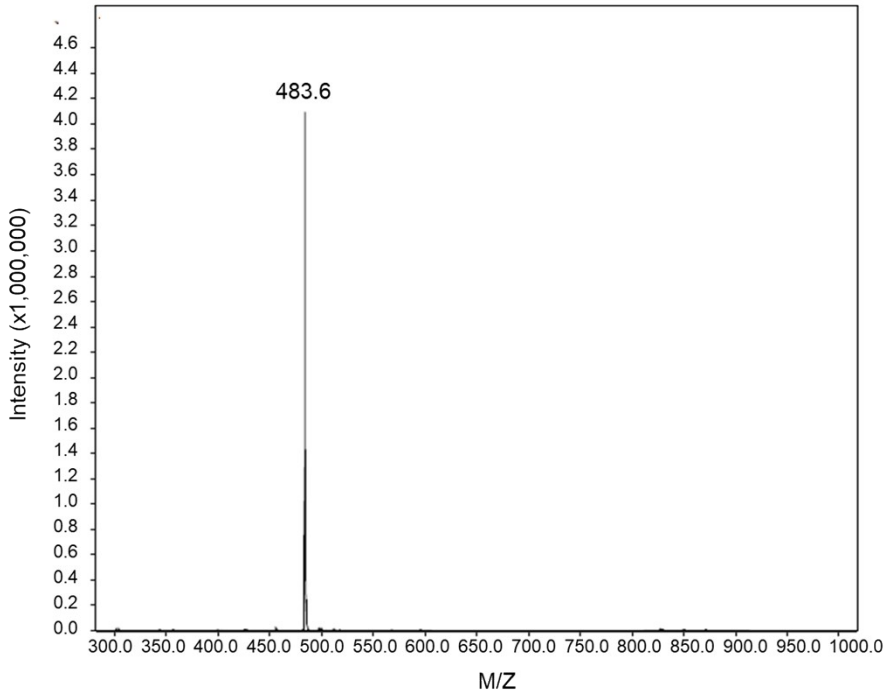

Figure S3. Mass spectrum in positive ion mode for $[P_{66614}][IR820]$

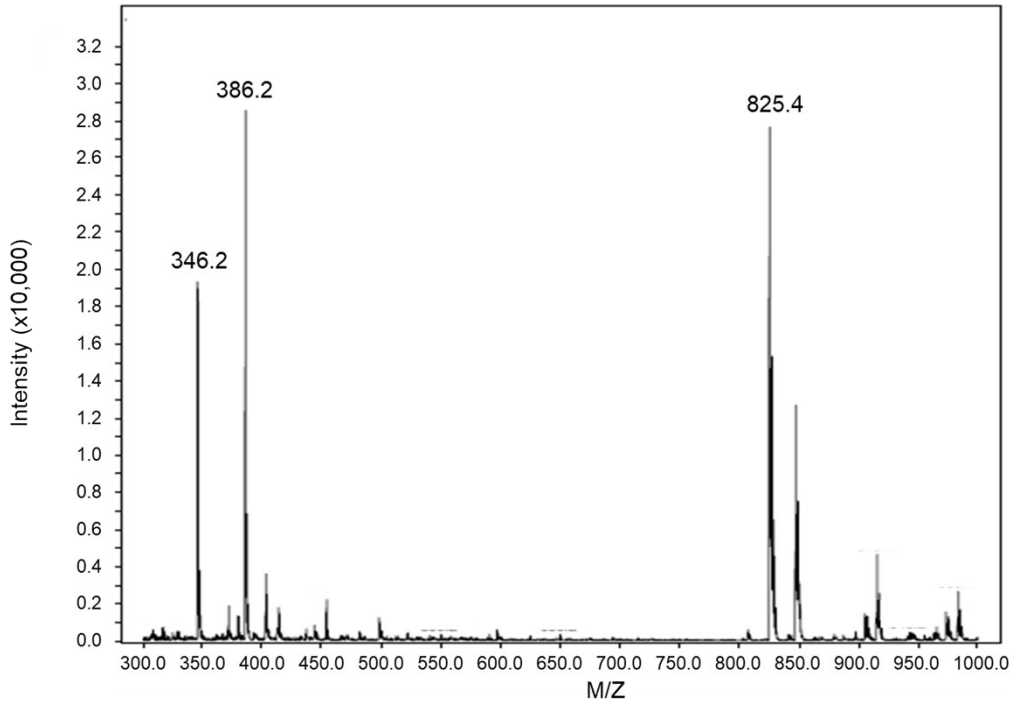

Figure S4. Mass spectrum in negative ion mode for $[P_{66614}][IR820]$

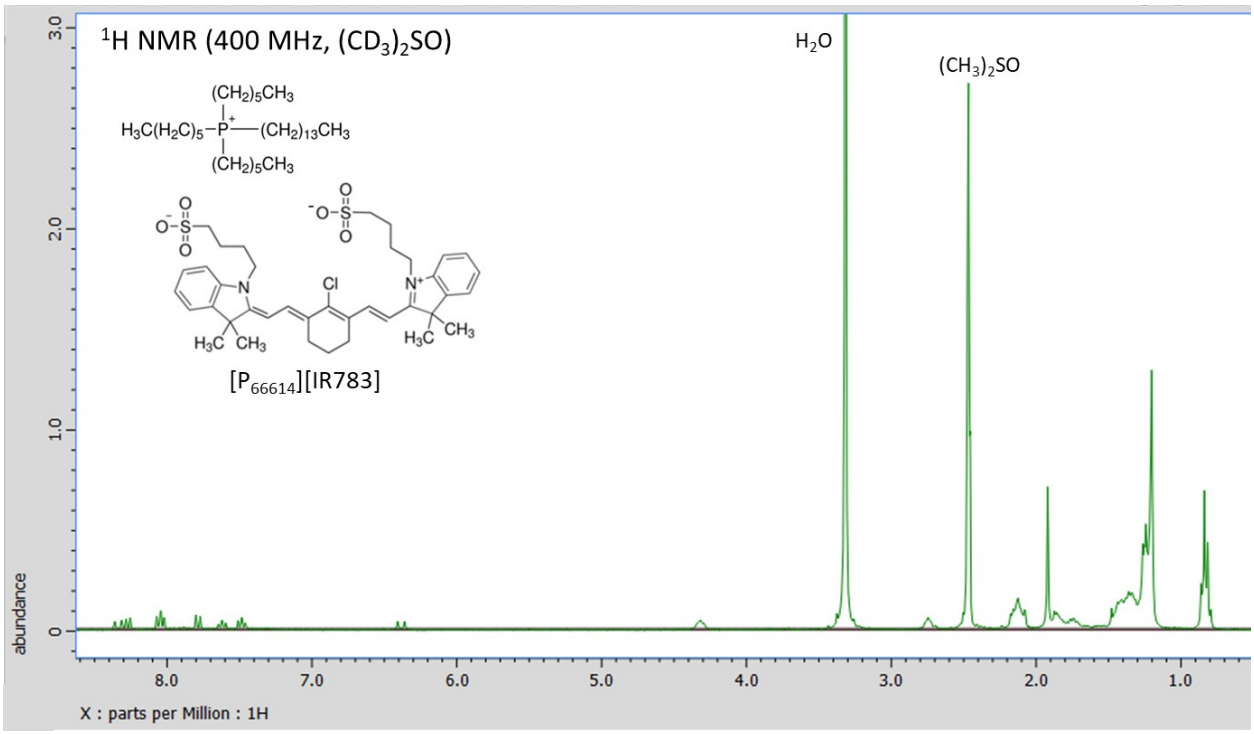

Figure S5. NMR spectrum of $[P_{66614}][IR783]$

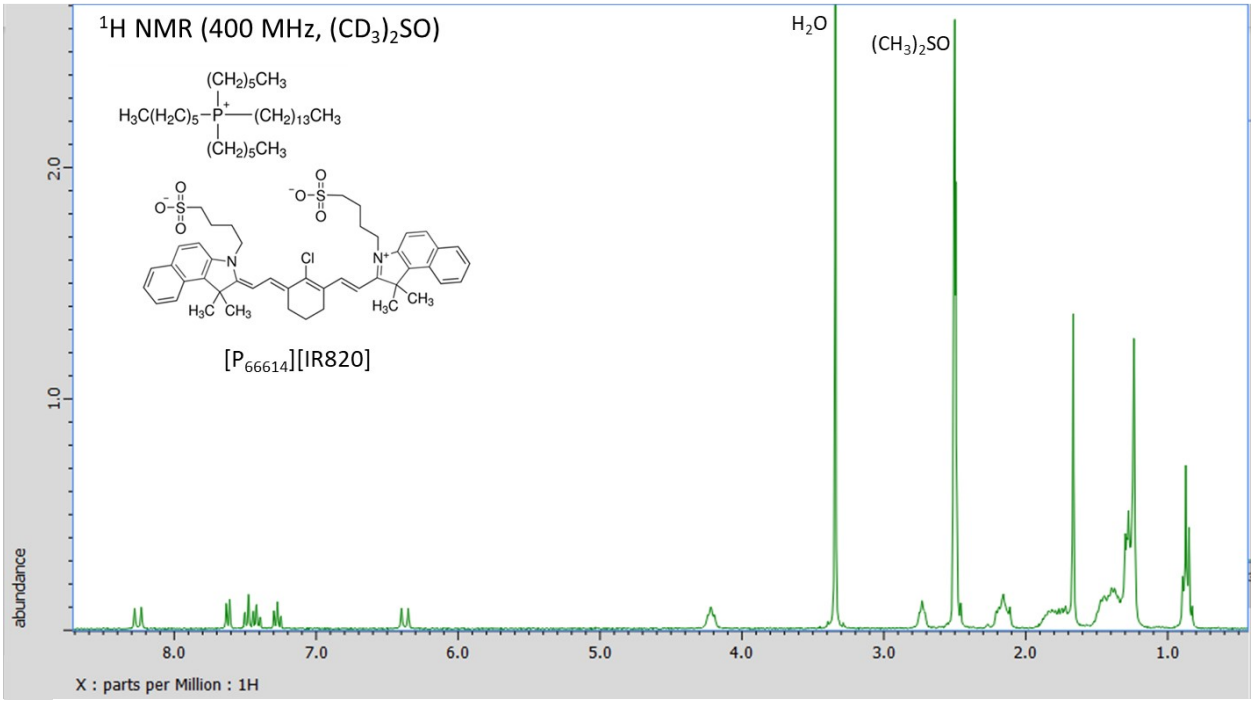

Figure S6. NMR spectrum of $[P_{66614}][IR820]$

Thermogravimetric analysis (TGA)

In PTT, the thermal stability of PTAs is a crucial factor.[1] Thermal stability of IMs compared to parent PTAs was analyzed using TGA measurements (Figure S3). For each sample, the temperature was scanned from 25 to 850 °C under uniform air flow at 10 °C ramp rate. IMs showed approximately 100% stability until 250 °C while parent compounds NaIR783 and NaIR820 exhibited 5-10% decomposition from 60 to 250 °C. More than one decomposition temperature was observed for all compounds. All compounds retain ~90% of their original mass at 300 °C. Onset temperature of decomposition (T_{onset}) was determined for IR820 and $[P_{66614}][IR820]$ and found to be 246.3 and 312.7 °C, respectively. Literature T_{onset} value for $[P_{66614}]Cl$ is shown to be 360 °C.[2] This is proof that conversion of free dyes to IMs enhanced their thermal stability as observed before for other IMs.[3] The second decompositions were observed around 450 °C and the final decomposition was recorded after 550 °C.

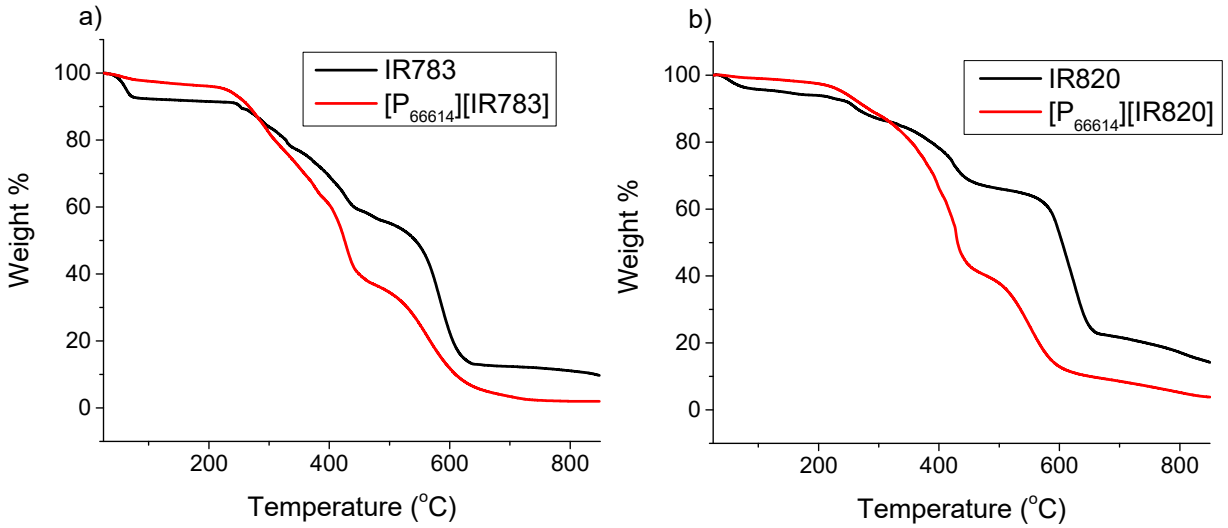

Figure S7. TGA profile of a) NaIR783 and $[P_{66614}][IR783]$ and b) NaIR820 parent dye and $[P_{66614}][IR820]$ IM

Molar extinction coefficients

Table S1. Molar extinction coefficients of NaIR783 and $[P_{66614}][IR783]$ in water and ethanol at a concentration of 5 μM.

λ (nm)	ε NaIR783 ethanol (M^{-1} cm^{-1})	ε NaIR783 aqueous (M^{-1} cm^{-1})	ε $[P_{66614}][IR783]$ IM ethanol (M^{-1} cm^{-1})	ε $[P_{66614}][IR783]$ INMs aqueous (M^{-1} cm^{-1})
784	385000	176000	331000	96250
718	102000	77200	87600	26600
λ (nm)	ε NaIR820 aqueous (M^{-1} cm^{-1})	ε NaIR820 ethanol (M^{-1} cm^{-1})	ε $[P_{66614}][IR820]$ (M^{-1} cm^{-1})	ε $[P_{66614}][IR820]$ nanoparticle (M^{-1} cm^{-1})
826	20300	174000	186000	24700
752	16200	55500	60900	68000

Photostability analysis

In PTT, the photostability of the PTA is an important factor to consider. The photostability of the NPs and IM were studied via excitation in kinetic mode for 1800 s and monitoring changes in fluorescence emission. Excitation wavelengths of 798, 785, and 786 nm were used to excite [P_{66614}][IR783] INMs in water, NaIR783 in ethanol, and [P_{66614}][IR783] combination IMs in ethanol respectively, and the fluorescence emission was monitored at 816 nm in ethanol and 800 nm in water. Excitation wavelengths of 837, 846, and 854 nm were used to excite [P_{66614}][IR820] INMs in water, NaIR820 in ethanol, and [P_{66614}][IR820] chemo-PTT combination IMs in ethanol respectively, and the fluorescence emission was monitored at 925 nm. NaIR783 dye shows some instability with fluorescence emission intensity decreased about 10% after 1800 s, IM and INMs based on NaIR783 show enhanced stability over the time interval (Figure S4). For NaIR820 and [P_{66614}][IR820] there was no significant change in the emission intensity after 1800 seconds of excitation, while the emission intensity is increased over time for INMs. The lack of decrease in emission indicates that IR820 is inherently a photostable compound and retains that trait when converted into IMs and NPs.

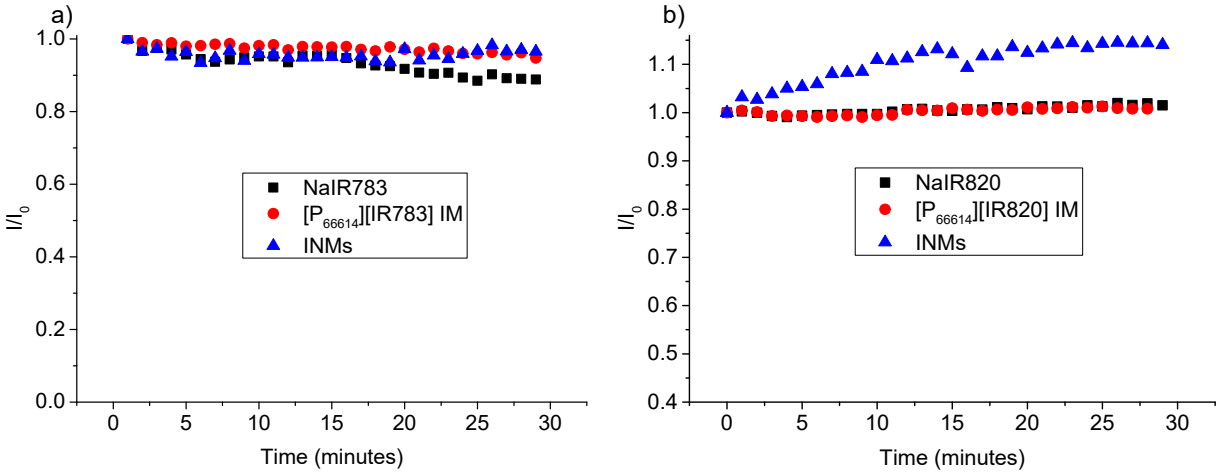

Figure S8. Photostability curves of a) IR783, [P_{66614}][IR783] IM, and [P_{66614}][IR783] INMs and b) IR820, [P_{66614}][IR820], and [P_{66614}][IR820] INMs over 30 min.

Quantum yield and photophysical rate constants

The quantum yield of IM and INMs were determined relative to the parent NaIR820 compound. The quantum yield is determined using a relative to a standard (NaIR820), as shown in **Equation S1**

$$\Phi_{un} = \Phi_s \times \frac{I_{un}}{I_s} \times \frac{Abs_s}{Abs_{un}} \times (\frac{n_{un}}{n_s})^2 \quad \text{(S1)}$$

where Φ_s is the quantum yield of the standard, I is the integrated emission intensity (830-1200 nm), Abs is the absorbance at the excitation wavelength (820 nm), and n is the refractive index of the standard (s) and unknown (un).

From the absorption and fluorescence emission spectra, the radiative rate constant (k_{rad}) was also calculated using the Stricker-Berg relationship (**Equation S2**)

$$k_{rad} = 2.88 \times 10^{-9} \times n^2 \times \frac{\int I(\tilde{\nu})d\tilde{\nu}}{\int I(\tilde{\nu})\tilde{\nu}^{-3}d\tilde{\nu}} \int \frac{\varepsilon(\tilde{\nu})}{\tilde{\nu}}d\tilde{\nu} \quad \text{(S2)}$$

where I is the emission intesity, $\tilde{\nu}$ is the wavenumber of light, and ε is the molar extinction coefficient.

Using the radiative rate constant, the non-radiative rate constant ($k_{non\text{-}rad}$) was calculated for each compound using **Equation S3**.

$$\Phi_F = \frac{k_{rad}}{k_{rad} + k_{non-rad}} \quad \text{(S3)}$$

Table S2. Photophysical rates of IR dyes and IMs in ethanol: quantum yield (Φ_F), radiative rate (k_{rad}), and non-radiative rate ($k_{non\text{-}rad}$).

Compound	Φ_F (%)	k_{rad}/s^{-1} x 10^6	$k_{non\text{-}rad}/s^{-1}$ x 10^8
NaIR783 in ethanol	4.30	4.19	16.7
$[P_{66614}][IR783]$ in ethanol	1.64	15.4	8.5
IR820 in ethanol	4.20	6.59	1.50

$[P_{66614}]$[IR820] in ethanol	4.82	7.75	1.53

Photothermal Efficiency

Photothermal heat conversion efficiencies (η) of the INMs and parent aqueous drugs were determined using the following Equation S4-S7.[4,5]

$$\eta = \frac{hs(T_{max} - T_{surr}) - Q_{dis}}{I(1 - 10^{-A})} \quad \text{(S4)}$$

Where h is the heat transfer coefficient, s is the surface area of the container, and hs is obtained from Equation S5 and Figure 4. T_{max} is the maximum steady state temperature of the INMs and for $[P_{66614}]$[IR783] INMs was 45.8 °C. The environmental temperature (T_{surr}) was 23.9 °C so the change in temperature (T_{max}-T_{surr}) for $[P_{66614}]$[IR783] suspension was determined to be 21.9 °C. I indicates the laser power, which was 1 W for all samples and A is the absorbance of PTA. Q_{dis} is the heat dissipated from lights absorbed by the solution and cuvette walls. Q_{dis} for INMs sample was determined from sample control with pure cell media and was found to be 17.2 mW. In order to determine hs, the following dimensionless parameter, θ, is introduced in Equation S5.

$$\theta = \frac{T - T_{surr}}{T_{max} - T_{surr}} \quad \text{(S5)}$$

Then, the time constant τ_s can be deduced from Equation S6.

$$t = -\tau_s \ln(\theta) \quad \text{(S6)}$$

Where t is time. τ_s of the $[P_{66614}]$[IR783] INMs sample was determined to be 155.5 s. By plugging this value into Equation S7, hs can be calculated.

$$hs = \frac{m_D C}{\tau_s} \quad \text{(S7)}$$

Where m_D is the mass of solution (1.0 g) and C is the specific heat (4.2 J/g °C). hs for $[P_{66614}][IR783]$ was calculated to be 27.1 mW/ °C. After substituting all parameters back into Equation S4, η was determined to be 44.6%.

ROS quantum yield

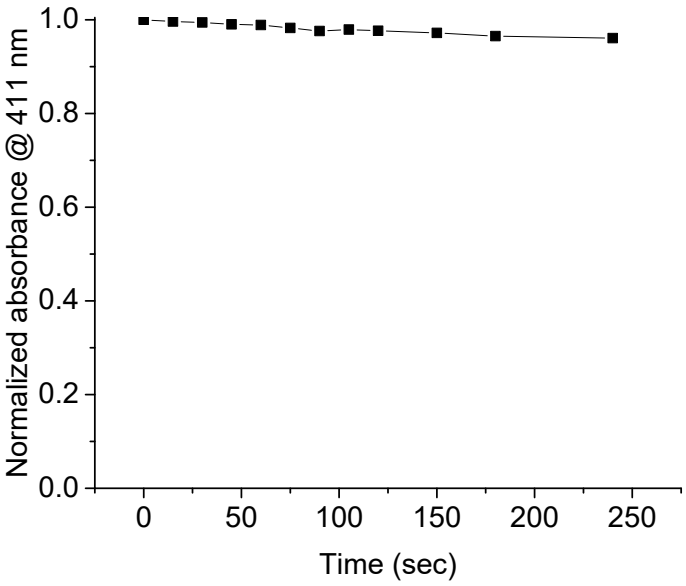

Figure S9. Normalized absorbance of DPBF probe (411 nm) in ethanol after irradiation with 808 nm laser

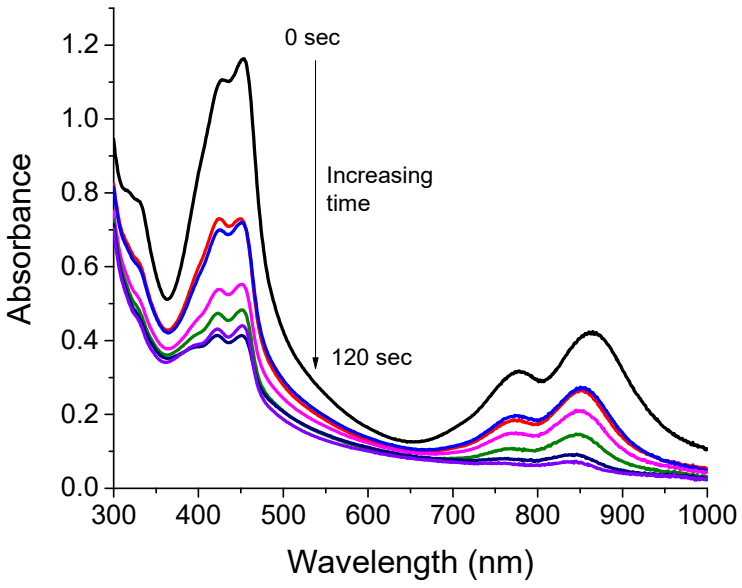

Figure S10. Photodegradation of DPBF upon increasing irradiation time in the presence of $[P_{66614}][IR820]$ in water

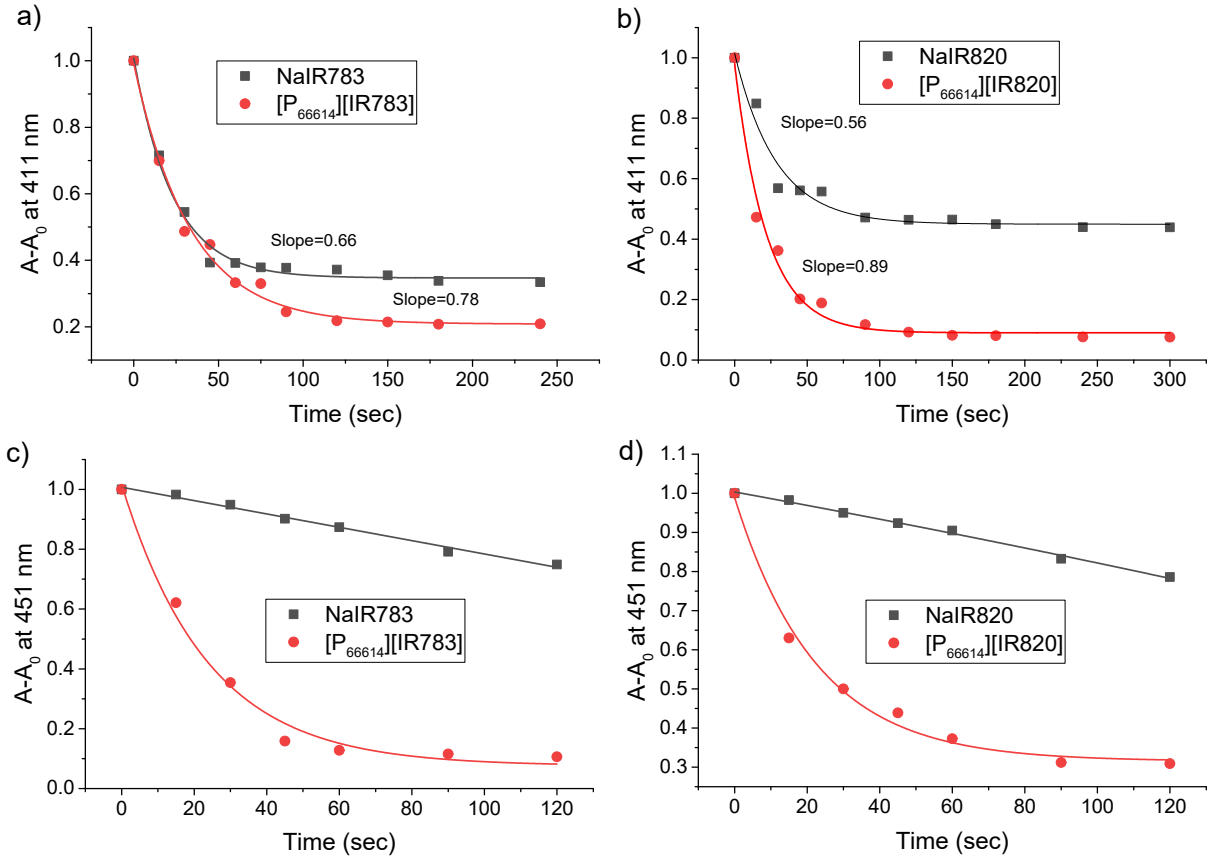

Figure S11. ROS QY results in ethanol of a) NaIR783 and $[P_{66614}][IR783]$ and b) NaIR820 and $[P_{66614}][IR820]$. ROS QY results in water of c) NaIR783 and $[P_{66614}][IR783]$ and d) NaIR820 and $[P_{66614}][IR820]$

In vitro Cytotoxicity

Table S3. 24 hr dark cytotoxicity (IC_{50}, μM) of cytotoxic IL, NIR dyes, and INMs in various cells lines: human breast cancer (MCF-7) and mouse breast cancer (4T1) where N/A is used in place of a numeric value indicating that it was nontoxic under experimental conditions.

Sample	**MCF-7**	**4T1**
NaIR783	45.29 ± 1.25	N/A
$[P_{66614}][IR783]$	4.76 ± 0.45	4.62 ± 0.55
NaIR820	N/A	N/A
$[P_{66614}][IR820]$	5.01 ± 0.31	3.09 ± 1.19
$[P_{66614}]Cl$	6.23 ± 0.24	6.75 ± 0.78

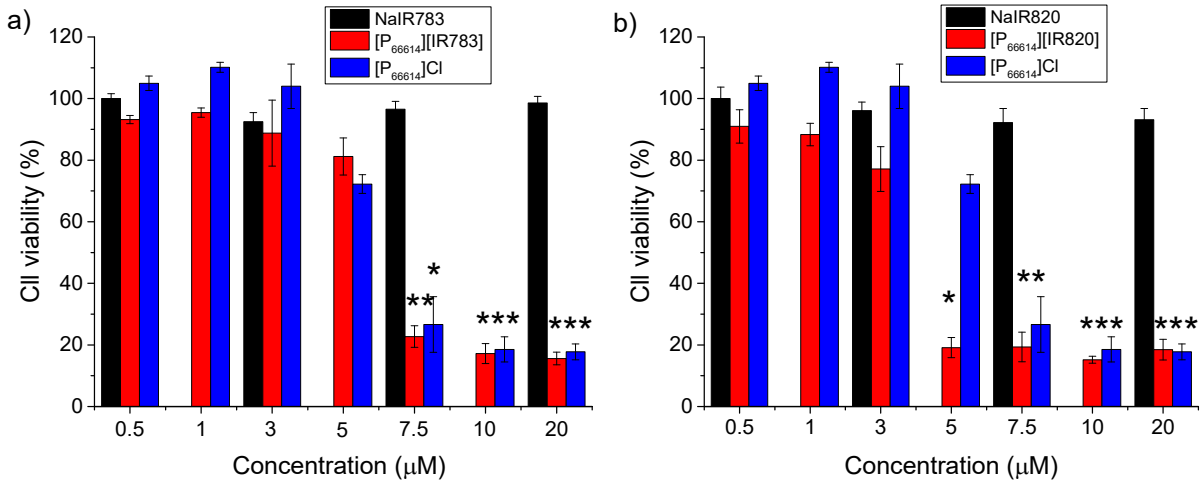

Figure S12. Cell viability plots for NIR dyes incubated with 4T1 cell line in the dark.

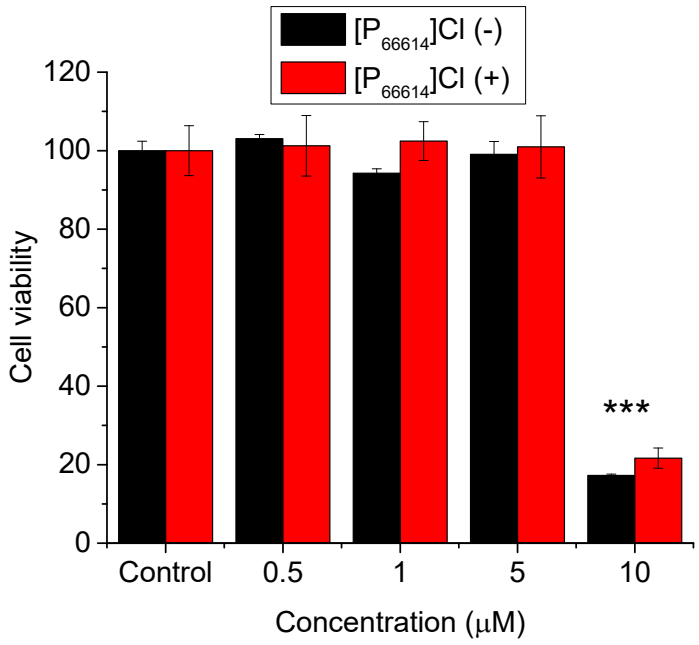

Figure S13. Cytotoxicity of $[P_{66614}]Cl$ incubated 4 hr in MCF-7 cells without irradiation (-) and upon irradiation with 808 nm laser (5 W/cm^2) for 5 min (+). P values are determined using two-tailed student's t-test and are reported as *p<0.05, **p<0.01, ***p<0.005.

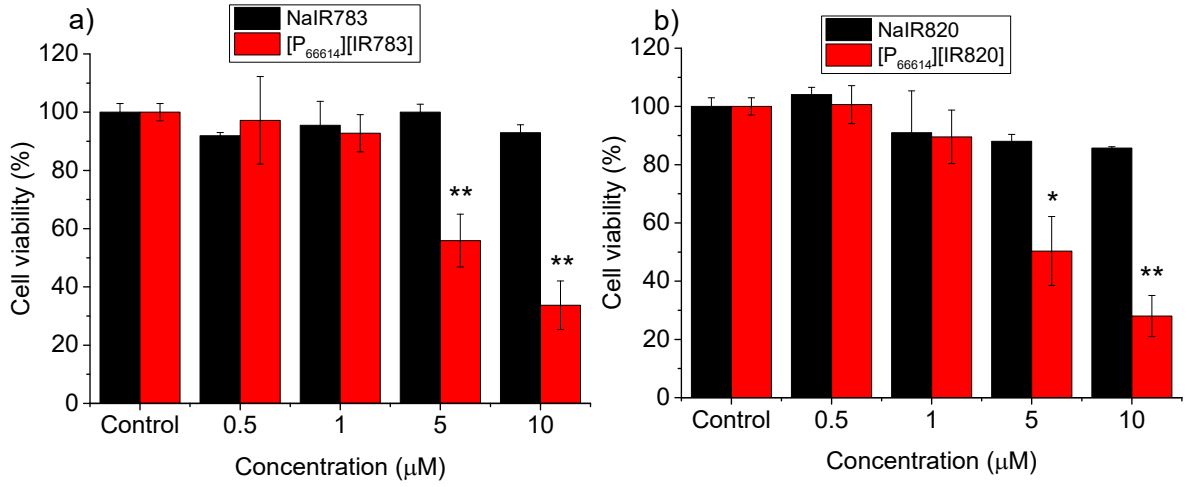

Figure S14. Cytotoxicity of (a) NaIR783 and $[P_{66614}][IR783]$ INMs and (b) NaIR820 and $[P_{66614}][IR820]$ INMs incubated 4 hr in MCF-7 cells and irradiated with 808 nm laser (1 W/cm^2) for 5 min. P values are determined using two-tailed student's t-test and are reported as *p<0.05, **p<0.01, ***p<0.005.

Table S4. Light cytotoxicity of NIR dyes and INMs in MCF-7 after 4 hr incubation and subsequent irradiation with 808 nm laser (1W/cm^2, 5 min) where N/A is used in place of a numeric value indicating that it was nontoxic under experimental conditions

Sample	**IC_{50} (μM)**
NaIR783	51.09 ± 0.77
[P_{66614}][IR783]	6.32 ± 1.39
NaIR820	53.90 ± 4.98
[P_{66614}][IR820]	5.42 ± 1.08

References

(1) Peng, H.; Tang, J.; Zheng, R.; Guo, G.; Dong, A.; Wang, Y.; Yang, W. Nuclear-Targeted Multifunctional Magnetic Nanoparticles for Photothermal Therapy. *Adv. Healthc. Mater.* **2017**, *6* (7), 1601289.

(2) Kolic, P. E.; Siraj, N.; Cong, M.; Regmi, B. P.; Luan, X.; Wang, Y.; Warner, I. M. Improving Energy Relay Dyes for Dye-Sensitized Solar Cells by Use of a Group of Uniform Materials Based on Organic Salts (GUMBOS). *RSC Adv.* **2016**, *6* (97), 95273–95282.

(3) Siraj, N.; Hasan, F.; Das, S.; Kiruri, L. W.; Steege Gall, K. E.; Baker, G. A.; Warner, I. M. Carbazole-Derived Group of Uniform Materials Based on Organic Salts: Solid State Fluorescent Analogues of Ionic Liquids for Potential Applications in Organic-Based Blue Light-Emitting Diodes. **2014**, *118* (5), 2312–2320.

(4) Tian, Q.; Jiang, F.; Zou, R.; Liu, Q.; Chen, Z.; Zhu, M.; Yang, S.; Wang, J.; Wang, J.; Hu, J. Hydrophilic Cu9S5 Nanocrystals: A Photothermal Agent with a 25.7% Heat Conversion Efficiency for Photothermal Ablation of Cancer Cells in Vivo. *ACS Nano* **2011**, *5* (12), 9761–9771.

(5) Liu, X.; Li, B.; Fu, F.; Xu, K.; Zou, R.; Wang, Q.; Zhang, B.; Chen, Z.; Hu, J. Facile Synthesis of Biocompatible Cysteine-Coated CuS Nanoparticles with High Photothermal Conversion Efficiency for Cancer Therapy. *Dalt. Trans.* **2014**, *43* (30), 11709–11715.